Calibration of a spinner anemometer for yaw misalignment measurements

Friis Pedersen, Troels; Demurtas, Giorgio; Zahle, Frederik

Published in:
Wind Energy

Link to article, DOI:
10.1002/we.1798

Publication date:
2015

Document Version
Publisher's PDF, also known as Version of record

Wind Energy

WIND ENERGY
Wind Energ. (2014)
Published online in Wiley Online Library (wileyonlinelibrary.com). DOI: 10.1002/we.1798

RESEARCH ARTICLE

Calibration of a spinner anemometer for yaw misalignment measurements

T. F. Pedersen, G. Demurtas and F. Zahle

Technical University of Denmark, Frederiksborgvej 399, PO Box 49, 4000 Roskilde, Denmark

ABSTRACT

The spinner anemometer is an instrument for yaw misalignment measurements without the drawbacks of instruments mounted on the nacelle top. The spinner anemometer uses a non-linear conversion algorithm that converts the measured wind speeds by three sonic sensors on the spinner to horizontal wind speed, yaw misalignment and flow inclination angle. The conversion algorithm utilizes two constants that are specific to the spinner and blade root design and to the mounting positions of the sonic sensors on the spinner. One constant, k_2, mainly affects the measurement of flow angles, while the other constant, k_1, mainly affects the measurement of wind speed. The ratio between the two constants, $k_\alpha = k_2/k_1$, however, only affects the measurement of flow angles. The calibration of k_α is thus a basic calibration of the spinner anemometer.

Theoretical background for the non-linear calibration is derived from the generic spinner anemometer conversion algorithm. Five different methods were evaluated for calibration of a spinner anemometer on a 500 kW wind turbine. The first three methods used rotor yaw direction as reference angular, while the wind turbine, was yawed in and out of the wind. The fourth method used a hub height met-mast wind vane as reference. The fifth method used computational fluid dynamics simulations. Method 1 utilizing yawing of the wind turbine in and out of the wind in stopped condition was the preferred method for calibration of k_α. The uncertainty of the yaw misalignment calibration was found to be 10%, giving an uncertainty of 1° at a yaw misalignment of 10°. © 2014 The Authors. *Wind Energy* published by John Wiley & Sons, Ltd.

KEYWORDS

anemometer; yaw misalignment; yaw error; flow inclination angle; nacelle anemometer; spinner anemometer; calibration

Correspondence

T. F. Pedersen, Wind Energy Department, DTU, Building 118, Frederiksborgvej 399, PO Box 49, 4000 Roskilde, Denmark.
E-mail: trpe@dtu.dk

Received 14 June 2013; Revised 7 May 2014; Accepted 25 July 2014

LIST OF SYMBOLS

F_1	calibration factor converting $k_{1,d}$ to k_1
F_2	calibration factor converting $k_{1,d}$ to k_1
F_α	calibration factor converting $k_{\alpha,d}$ to k_α
k_1	algorithm and calibration constant mainly related to wind speed measurements
$k_{1,d}$	default algorithm constant mainly related to wind speed measurements
k_2	algorithm constant mainly related to angular measurements
$k_{2,d}$	default algorithm constant mainly related to angular measurements
k_α	angular measurement calibration constant equal to k_2/k_1
$k_{\alpha,d}$	default angular measurement calibration constant equal to $k_{2,d}/k_{1,d}$
U	wind speed vector modulus
U_{hor}	horizontal wind speed (calibrated)
$U_{hor,d}$	horizontal wind speed (measured with $k_{1,d}$ and $k_{2,d}$)
$U_{hor,d,c}$	horizontal wind speed (calibrated with correct k_α but not correct k_1)

$U_{x,n}$	horizontal wind speed component along nacelle x-axis
$U_{y,n}$	horizontal wind speed component transversal to shaft axis
$U_{z,n}$	vertical wind speed component
V_1	wind speed along sonic sensor path 1
V_2	wind speed along sonic sensor path 2
V_3	wind speed along sonic sensor path 3
V_{ave}	average wind speed of sonic sensors
α	wind inflow angle relative to the shaft axis
β	flow inclination angle relative to horizontal (positive when upwards)
γ	yaw misalignment defined as wind direction minus turbine yaw direction
γ_{ref}	reference yaw misalignment (calculated as mast wind direction minus wind turbine yaw direction)
δ	shaft tilt angle
ϕ	rotor azimuth position (equal to zero when sonic sensor 1 is at top position, positive clockwise seen from the front of the wind turbine)
θ	spinner azimuth position of flow stagnation point (relative to sonic sensor 1)
θ_{dir}	wind direction measured at the met mast, referred to geographical north
$\theta_{dir,10}$	10 min average of θ_{dir}
θ_{yaw}	yaw direction of the wind turbine nacelle, measured by the yaw position sensor
$\theta_{yaw,10}$	10 min average of θ_{yaw}.
$\overline{\theta_{dir}}$	mean wind direction during the calibration test, referred to the yaw position sensor

1. INTRODUCTION

A challenge in wind turbine design is how to achieve an accurate and cheap measurement of the wind that flows into the wind turbine rotor. An accurate knowledge of the incoming wind is important in order to regulate yaw and pitch for optimized power, without being jeopardized by higher rotor loads or noise. Nacelle anemometry is used in wind turbine yaw control to measure wind speed and wind direction by cup anemometers and wind vanes or 2D sonic anemometers, mounted on top of the nacelle. Nacelle-mounted sensors are, however, influenced significantly by flow distortion from blade root sections and by a range of other sources, see the work of Frandsen *et al.*[1] Computational fluid dynamics (CFD) calculations confirm the sensitivity to flow distortion on the turbine nacelles.[2] The flow distortion is normally corrected for in the control systems, often based on a wind speed dependent function. However, mounting and adjustments of the wind sensors might introduce large yaw misalignments if not made with high precision in mounting, adjustment and calibration. Variations in the flow inclination angle due to terrain slope or swirl of wakes of other wind turbines may also influence on the efficiency of nacelle-based wind direction sensors. Inefficient yaw misalignment measurements lead to loss of energy.[3]

An alternative to nacelle anemometry is spinner anemometry,[4] which measures yaw misalignment without offset or mounting and alignment errors. This type of wind sensor utilizes sonic sensor technology; the same technology used on 2D sonic anemometers on nacelles today. The spinner anemometer integrates three surface mounted 1D sonic sensors (Figure 1) with the spinner of a wind turbine and utilizes the flow over the spinner. The three 1D sonic sensors detect direc-

Figure 1. A 1D sonic sensor normally mounted from the inside of the spinner.

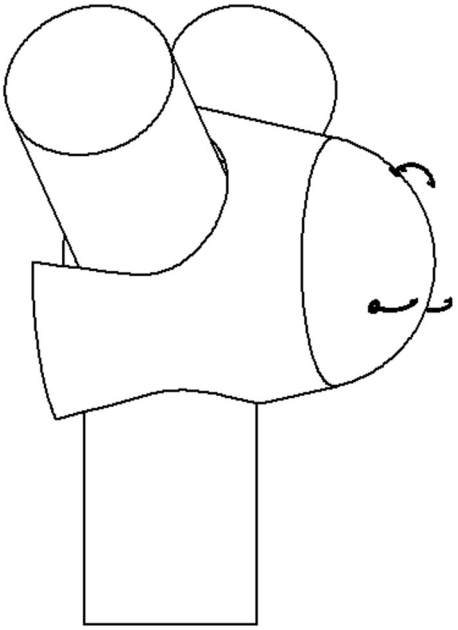

Figure 2. A spinner anemometer with three sonic sensors.

tional wind speeds in three positions over the spinner surface, while the wind component due to rotation is out-compensated as the sonic sensor paths are perpendicular to the velocity component due to rotation (Figure 2).

In axial flow with the flow stagnation point directly on the nose centre, all sonic sensors measure the same wind speed. In skew air flow, the stagnation point moves away from the nose. A sonic sensor closer to the stagnation point experiences reduced wind speed, while a sensor further away experiences increased wind speed. This results in a sinusoidal variation in wind speed seen by each sonic sensor during rotation.

The spinner anemometer includes an algorithm to transform the wind speeds measured by the three sonic sensors to horizontal wind speed, yaw misalignment and flow inclination angle.[5] The algorithm utilizes two spinner anemometer constants, k_1 and k_2. These are specific to the design of the spinner and blade roots and the mounting of the sonic sensors on the spinner. The two constants must be calibrated in order to measure the wind accurately at the spinner. The constants are considered to represent free wind speed measurements when the wind turbine is stopped and the rotor is pointing into the wind. During operation, the measurements represent the wind at the spinner as it is disturbed by the induced wind speed due to the rotor, and this will cause measurements at the spinner to deviate from free wind measurements. If the induced wind speed is known, then corrections can be made to convert wind conditions at the spinner to free wind conditions.

When default constants, $k_{1,d}$ and $k_{2,d}$, are inserted in the spinner anemometer box, the spinner anemometer can still measure wind speed, yaw misalignment and flow inclination angle in the same way a cup anemometer can measure wind speed without applying the calibration constants on beforehand. In this case, the measurements must be corrected with the right calibration constants after measurements have been made. For a spinner anemometer with a non-linear conversion algorithm, this correction is more complicated than for a cup anemometer. However, if the spinner anemometer is calibrated in the sequence—internal calibration, calibration for angular measurements, calibration of wind speed—then measured wind speeds can be converted linearly, like for cup anemometers. Calibration for angular measurements is thus an important calibration in the calibration chain, not just for yaw misalignment and flow inclination angle measurements but also for wind speed measurements. This article will focus on the correct calibration for angular measurements when the influence of the non-linear conversion algorithm is taken into account. A practical example that includes and evaluates different methods is provided.

2. THE SPINNER ANEMOMETER CONVERSION ALGORITHM

The spinner anemometer conversion algorithm[5] transforms the measured wind speeds of the three sonic sensors to the horizontal wind speed, the yaw misalignment and the flow inclination angle. The algorithm is revisited here for the overall understanding of the measurement principle and for clarification of the transformations back and forth, which are used in the calibration data analysis to derive the correct calibration factor. We first set up a coordinate system.

2.1. Coordinate systems

The coordinate systems for transforming the spinner anemometer parameters from the rotating spinner to the fixed nacelle are shown in Figure 3. The inflow angle α, which is not directly shown, is the angle between the shaft axis and the vector of the inflow wind speed U. The yaw misalignment γ is defined as the wind direction minus the yaw direction (equation (1)).

$$\gamma = \theta_{dir} - \theta_{yaw} \tag{1}$$

2.2. Generic spinner anemometer wind speed relations

The basic spinner anemometer measurements consist of the three sonic sensor wind speeds V_1, V_2 and V_3, and the rotor azimuth position ϕ. The azimuth position is derived from accelerometers, mounted in each foot of the sonic sensors. The generic equations that relate these measurements to the vector wind speed U, the inflow angle relative to the shaft axis α and the azimuth position of the flow stagnation point on the spinner θ are, as derived in the work of Pedersen,[4] as follows:

$$V_1 = U(k_1 \cos\alpha - k_2 \sin\alpha \cos\theta) \tag{2}$$

$$V_2 = U\left(k_1 \cos\alpha - k_2 \sin\alpha \cos\left(\theta - \frac{2\pi}{3}\right)\right) \tag{3}$$

$$V_3 = U\left(k_1 \cos\alpha - k_2 \sin\alpha \cos\left(\theta - \frac{4\pi}{3}\right)\right) \tag{4}$$

The generic equations include the two spinner anemometer algorithm constants k_1 and k_2.

2.3. Transformation from sonic sensor measurements to spinner anemometer parameters

The sonic sensor wind speeds V_1, V_2 and V_3 and the rotor azimuth position ϕ measurements are converted (Figure 4) to the spinner anemometer output parameters, horizontal wind speed U_{hor}, yaw misalignment γ and flow inclination angle β, in a number of steps.

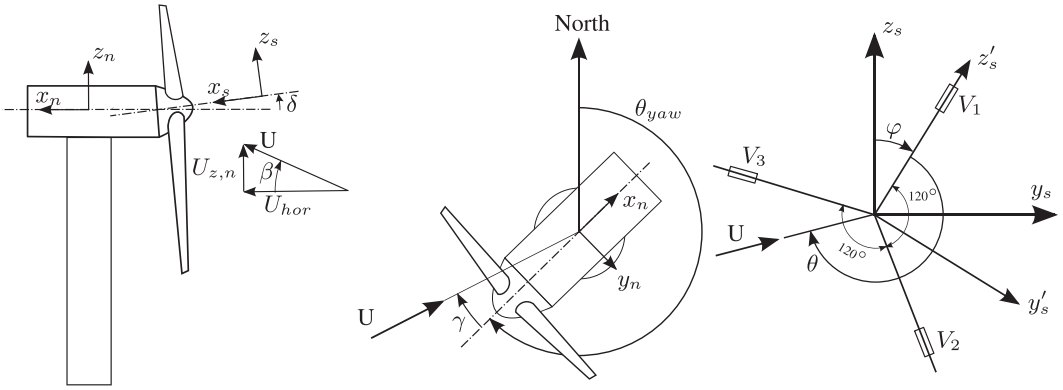

Figure 3. Coordinate systems and definition of angles: rotating spinner coordinate system (x'_s, y'_s, z'_s), non-rotating shaft coordinate system (x_s, y_s, z_s), fixed nacelle coordinate system (x_n, y_n, z_n), yaw direction θ_{yaw}, yaw misalignment γ, flow inclination angle β, tilt angle δ, azimuth position of flow stagnation point on spinner θ (relative to sonic sensor 1), rotor azimuth position ϕ (position of sonic sensor 1 relative to vertical). (a) Side view, (b) top view and (c) front view along the shaft axis.

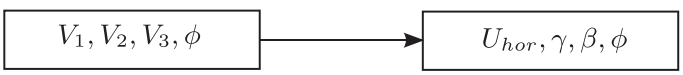

Figure 4. Direct transformation from sonic sensor wind speed to spinner anemometer parameters.

The first step in the transformation relates the sonic sensor wind speeds to the vector wind speed U, the inflow angle relative to the shaft axis α and the azimuth position of the flow stagnation point θ in the rotating spinner coordinate system of Figure 3. The inflow angle relative to the rotor axis is

$$\alpha = \arctan\left(\frac{k_1\sqrt{3(V_1 - V_{ave})^2 + (V_2 - V_3)^2}}{\sqrt{3}k_2 V_{ave}}\right) \tag{5}$$

where the average of the sonic sensor wind speeds is

$$V_{ave} = \frac{1}{3}(V_1 + V_2 + V_3) \tag{6}$$

The module of the vector wind speed is

$$U = \frac{V_{ave}}{k_1 \cos\alpha} \tag{7}$$

And the flow stagnation azimuth position is*

$$\theta = \arctan\left(\frac{V_2 - V_3}{\sqrt{3}(V_1 - V_{ave})}\right) + \pi \tag{8}$$

The second step transforms the parameters in the spinner coordinate system to three wind speed components in the non-rotating shaft coordinate system. The wind speed component along the x_s-axis is

$$U_{x,s} = U\cos\alpha \tag{9}$$

The combined wind speed component perpendicular to the x_s-axis is

$$U_\alpha = U\sin\alpha \tag{10}$$

The wind speed component along the y_s-axis is

$$U_{y,s} = -U_\alpha \sin(\phi + \theta) \tag{11}$$

where ϕ is the measured rotor azimuth position. The wind speed component along the z_s-axis is

$$U_{z,s} = -U_\alpha cos(\phi + \theta) \tag{12}$$

The third step transforms the three wind components in the non-rotating shaft coordinate system to three wind speed components in a fixed nacelle coordinate system, where the y_n-axis is horizontal and parallel with the y_s-axis, the x_n-axis is horizontal and the z_n-axis is vertical, and δ is the shaft tilt angle.

$$U_x = U_{x,s}\cos\delta + U_{z,s}\sin\delta \tag{13}$$

$$U_y = U_{y,s} \tag{14}$$

$$U_z = U_{z,s}\cos\delta - U_{x,s}\sin\delta \tag{15}$$

With the fourth and last step, these wind speed components, similar to a standard 3D sonic anemometer, are transformed to the spinner anemometer output parameters. The horizontal wind speed is

$$U_{hor} = \sqrt{U_x^2 + U_y^2} \tag{16}$$

The yaw misalignment:

$$\gamma = \arctan\left(\frac{U_y}{U_x}\right) \tag{17}$$

And the flow inclination angle:

$$\beta = \arctan\left(\frac{U_z}{U_{hor}}\right) \tag{18}$$

*Because of the properties of the arctangent function (which is the inverse of the tangent only in the first and fourth quadrant), we use the computed function 'atan2', which is available in most programming languages, in all equations. This function takes all quadrants into account, including the singularity where the denominator is equal to zero. The $+\pi$ is necessary to make the position of the stagnation point consistent with the sign of the velocity components along the axis y_s and z_s.

2.4. Transformation from spinner anemometer parameters back to sonic sensor wind speeds

In order to correct measured spinner anemometer data with calibrated spinner anemometer constants, it is necessary to reverse the spinner anemometer algorithm. This inverse transformation to the sensor path speeds is presented in Figure 5. A special consideration of the rotor position ϕ has to be given because the rotor position is not an output parameter of the spinner anemometer.

The first step of the inverse transformation transforms the spinner anemometer output parameters U_{hor}, γ and β to the sonic sensor wind speed components U_x, U_y and U_z in the nacelle coordinate system:

$$U_x = U_{hor} \cos \gamma \tag{19}$$

$$U_y = U_{hor} \sin \gamma \tag{20}$$

$$U_z = U_{hor} \tan \beta \tag{21}$$

The second inverse step transforms the wind speed components in the nacelle coordinate system to wind speed components in the shaft coordinate system:

$$U_{x,s} = U_x \cos \delta - U_z \sin \delta \tag{22}$$

$$U_{y,s} = U_y \tag{23}$$

$$U_{z,s} = U_x \sin \delta + U_z \cos \delta \tag{24}$$

The third inverse step transforms the wind speed components in the shaft coordinate system to wind parameters in the spinner coordinate system. The rotor azimuth position is not important for transformations back and forth and can be set equal to zero. The vector wind speed and the inflow angle to the shaft are:

$$U = \sqrt{U_{x,s}^2 + U_{y,s}^2 + U_{z,s}^2} \tag{25}$$

$$U_\alpha = \sqrt{U_{y,s}^2 + U_{z,s}^2} \tag{26}$$

$$\alpha = \arctan\left(\frac{U_\alpha}{U_{x,s}}\right) \tag{27}$$

And now, using the rotor azimuth position to find the flow stagnation azimuth position,

$$\theta = \arctan\left(\frac{U_{y,s}}{U_{z,s}}\right) - \phi + \pi \tag{28}$$

Finally, the fourth inverse step transforms the wind parameters in the spinner coordinate system to the sonic sensor wind speeds:

$$V_1 = U\,(k_1 \cos \alpha - k_2 \sin \alpha \cos \theta) \tag{29}$$

$$V_2 = U\left(k_1 \cos \alpha - k_2 \sin \alpha \cos\left(\theta - \frac{2\pi}{3}\right)\right) \tag{30}$$

$$V_3 = U\left(k_1 \cos \alpha - k_2 \sin \alpha \cos\left(\theta - \frac{4\pi}{3}\right)\right) \tag{31}$$

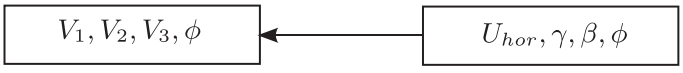

Figure 5. Inverse transformation, from spinner anemometer parameters to sonic sensors wind speeds.

3. CORRECTION FACTORS FOR CORRECTION OF SPINNER ANEMOMETER CONSTANTS

In the calibration process, correction factors (denoted by F) are multiplied to the default constants $k_{1,d}$ and $k_{2,d}$ that are inserted into the spinner anemometer box before calibration to obtain the calibrated k_1 and k_2 constants:

$$k_1 = F_1 k_{1,d} \tag{32}$$

$$k_2 = F_2 k_{2,d} \tag{33}$$

In calibration for angular measurements, the calibration factor $F_\alpha = F_2/F_1$ is determined. F_α is used to set k_2 equal to

$$k_2 = F_\alpha k_{2,d} \tag{34}$$

while $k_1 = k_{1,d}$ is kept constant. The k_2 value shall be set in the spinner anemometer box as soon as the calibration for angular measurements have been made. The spinner anemometer should be operated with default calibration constants only for a minimum of time required to collect measurements needed for determination of F_α.

The correction factors are derived by combining the generic spinner anemometer wind speed relations. Firstly, equations (2) and (3) are rewritten with respect to U and equalled, and α is extracted:

$$\tan\alpha = \frac{\sin\alpha}{\cos\alpha} = \frac{k_1}{k_2}\frac{V_2 - V_1}{V_2\cos\theta - V_1\cos\left(\theta - \frac{2\pi}{3}\right)} \tag{35}$$

As seen, the measured inflow angle depends on the position of the stagnation point θ, the wind speed at the sonic sensor paths (V_1 and V_2), and the ratio between the two spinner anemometer constants, which is now, for convenience, defined as

$$k_\alpha = \frac{k_2}{k_1} \tag{36}$$

Then,

$$\alpha = \arctan\left(\frac{V_2 - V_1}{k_\alpha\left(V_2\cos\theta - V_1\cos\left(\theta - \frac{2\pi}{3}\right)\right)}\right) \tag{37}$$

It is now clear that the angular measurement is only dependent on k_α. It is thus only necessary to calibrate this value for correct measurements of yaw misalignment and flow inclination angle. We can now introduce the correction factor that relates the constants to the situations before and after the calibration. Some of the variables are not affected by the calibration, while others are. For those affected by the calibration, the subscript d is used to reference default conditions before calibration. The measurements of wind speed in the sensor paths are not affected by a calibration. Therefore, V_1, V_2, V_3 before and after calibration are unchanged, and the position of the stagnation point θ is unchanged (equation (8)).

The inflow angle α, calculated by the spinner anemometer algorithm, is affected by the calibration. Using equation (37) and extracting k_α for conditions before and after calibration, we get

before calibration,

$$k_{\alpha,d} = \frac{V_2 - V_1}{\tan\alpha_d\left(V_2\cos\theta - V_1\cos\left(\theta - \frac{2\pi}{3}\right)\right)} \tag{38}$$

after calibration,

$$k_\alpha = \frac{V_2 - V_1}{\tan\alpha\left(V_2\cos\theta - V_1\cos\left(\theta - \frac{2\pi}{3}\right)\right)} \tag{39}$$

The correction factor for angular calibration is then

$$F_\alpha = \frac{k_\alpha}{k_{\alpha,d}} = \frac{\tan\alpha_d}{\tan\alpha} = \frac{F_2}{F_1} = \frac{k_{1,d}k_2}{k_1 k_{2,d}} \tag{40}$$

F_α is seen to be independent of wind speeds. It is possible to determine F_α by angular relations alone and then derive the correct inflow angle α relative to the shaft axis. When this angle is correct, the derived yaw misalignment and flow inclination angles will also be calculated correctly.

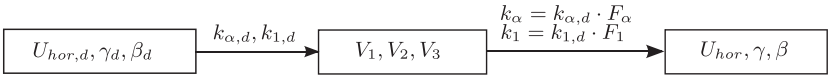

Figure 6. Application of correction factors to data measured with default calibration constants. For calibration for angular measurements, only F_1 is set equal to 1.

The calibration of k_1 can be determined by considering the wind speed U_d, calculated by the spinner anemometer algorithm before calibration, and the wind speed U after calibration. By rewriting the difference between equations (2) and (3), we can isolate k_2:

before calibration,

$$k_{2,d} = \frac{V_1 - V_2}{U_d \sin\alpha_d \left(\cos\left(\theta - \frac{2\pi}{3}\right) - \cos\theta\right)} \tag{41}$$

after calibration,

$$k_2 = \frac{V_1 - V_2}{U_d \sin\alpha \left(\cos\left(\theta - \frac{2\pi}{3}\right) - \cos\theta\right)} \tag{42}$$

The correction factor F_2 is then

$$F_2 = \frac{k_2}{k_{2,d}} = \frac{U_d \sin\alpha_d}{U \sin\alpha} \tag{43}$$

The correction factor F_1 is obtained by combining equation (36) with (43):

$$F_1 = \frac{F_2}{F_\alpha} = \frac{U_d \sin\alpha_d}{U \sin\alpha} \frac{\tan\alpha}{\tan\alpha_d} = \frac{U_d \cos\alpha_d}{U \cos\alpha} \tag{44}$$

It is seen that the correction factor F_1 becomes a clean wind speed correction factor when $\alpha = \alpha_d$. This is the case when angular calibration and insertion of the calibrated value into the spinner anemometer box ($k_2 = F_\alpha k_{2,d}$ while $k_1 = k_{1,d}$) has been made prior to wind speed calibration. When calibration of wind speed is made, then we can insert the new corrections in the spinner anemometer box: $k_1 = F_1 k_{1,d}$ and $k_2 = F_1 k_{2,d}$.*

4. APPLICATION OF CORRECTION FACTORS ON MEASUREMENTS MADE WITH DEFAULT SPINNER ANEMOMETER CONSTANTS

When a spinner anemometer is mounted on a spinner of a new wind turbine type, the spinner anemometer constants are set as default constants (for example, $k_\alpha = 1$ and $k_1 = 1$). When data are acquired with default spinner anemometer constants, then data must be converted with the inverse and forward transformations described in Sections 2.4 and 2.3, respectively, in that order to avoid conversion errors. This is the case for the analysis of the calibration data in order to determine the correction factor F_α and F_1 to correct the default constants. This is also the case when measured data without applied calibration spinner anemometer constants have to be converted to calibrated data.† The measured data are corrected completely without conversion errors by the procedure in Figure 6, which uses the conversion procedures developed in Section 3.

For the second step, right of Figure 6, the rotor azimuth position ϕ is not known from the spinner anemometer output when the output mode is in 'normal mode' (see the manual of the Spinner anemometer[6]). For the further correction, the rotor azimuth position is set equal to a constant value, for example, zero. This is only reasonable as long as the spinner anemometer has had an internal calibration to take account of all geometric deviations in spinner and sensor paths.[6] This internal calibration assures that all three sonic sensors measure the same wind speeds during rotation, keeping the average wind speed of the three sensors the same. In this way, we do not derive the actual measured sonic sensor wind speeds for the actual rotor azimuth position, but the ones we derive are equivalent to the measured sonic sensor wind speeds with respect to the conversion to calibrated spinner anemometer data. The flow stagnation azimuth position on the spinner is under these assumptions determined from equation (28) and is correct.

*Note the suffix d is here used for conditions before wind speed calibration but after angular measurement calibration.

†It is always preferred to calibrate F_α first and correct k_2 and then calibrate F_1 and correct k_1 and k_2 in the second step before actual measurements are made in order to minimize linearization effects.

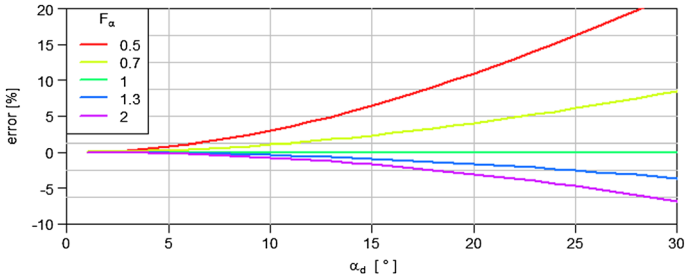

Figure 7. Error due to linearization of the conversion function, equation (46).

4.1. Errors due to linearization effects

The conversion in Figure 6 should be applied to the raw fast scanned data and will give correct results, also when data are afterwards averaged over time. However, if we consider 10 min averaged data where the F_α correction factor has not been applied, the non-linearity of the conversion algorithm results in deviations. To get an estimate of this deviation, we consider a simple case. We neglect the tilt angle (setting $\delta = 0$) and assume the flow inclination angle equal to zero (setting $\beta = 0$). Then, we can derive an expression of the calibrated yaw misalignment as function of the default yaw misalignment:

$$\alpha = \arctan\left(\frac{1}{F_\alpha}\tan\alpha_d\right) \tag{45}$$

The expression of equation (45) is non-linear, which means that averaged values introduce a deviation. As an example, the deviation of a converted default measured yaw misalignment of 10° and a standard deviation of 5°, and with a conversion factor F_α of 0.7 is −0.7% (converted value 14.04° instead of 14.14°), while the deviation is +0.3% for an F_α value of 1.3 (converted value 7.748° instead of 7.724°). The deviation seems rather constant for different yaw misalignment angles but is reduced for smaller standard deviations. The deviation increases almost exponentially with the distance of F_α from 1.0. For many cases, this deviation is small enough to be neglected, but it should be emphasized that the deviations are eliminated if the calibration of F_α is made before angular measurements are made.

In case we also linearize the conversion of raw fast scanned data to reduce computational and implementation efforts, we introduce another linearization error. When we linearize equation (45), we get

$$\alpha_{lin} = \frac{\alpha_d}{F_\alpha} \tag{46}$$

The error in estimation of F_α by linearization is shown in percentage in Figure 7. The error is seen to be small for correction factors close to 1.0 and also for small yaw misalignments, while for larger yaw misalignments, the error becomes significant.

5. CALIBRATION OF THE CORRECTION FACTOR F_α FOR A SPINNER ANEMOMETER ON A STALL-REGULATED 500 KW WIND TURBINE

The following example of calibration of F_α for angular measurements uses the inverse and forward transformations from Sections 2.4 and 2.3. A spinner anemometer is mounted on a 500 kW stall-regulated wind turbine, described by Paulsen[7] (Figure 8). Two of the three sonic sensors are seen on the spinner; the one on the top indicating the sonic sensor path in which the wind speed is measured.* After mounting of the spinner anemometer sonic sensors and the conversion box on the spinner, the tilt angle of the rotor shaft and the default spinner anemometer constants $k_{1,d} = k_{2,d} = 1.0$ were set in the spinner anemometer box. An internal calibration was then made according to the operation manual.[6] The internal calibration was activated and made during operation and was made in less than an hour. The internal calibration must be made prior to the F_α calibration to avoid uncertainties due to the rotor azimuth position and also to avoid 1P variations in the measurements. The internal calibration is made under the precondition that all three sonic sensors measure the same average wind speed over time.

The calibration of F_α consists in finding the value where the yaw misalignment indicated by the spinner anemometer effectively corresponds to the yaw misalignment of the wind turbine as defined in equation (1). The calibration can be

*Note the backwards tilting of the sonic sensor path relative to the local flow in order to avoid sensor head flow distortion.

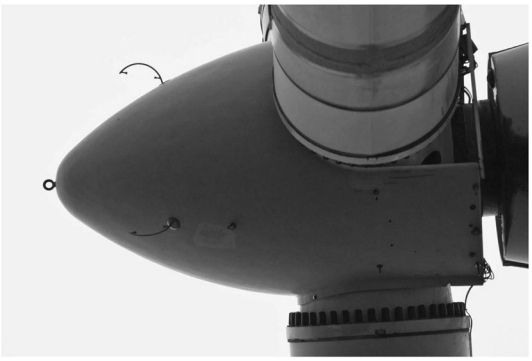

Figure 8. The spinner anemometer on a Nordtank 500 kW wind turbine.

made in several ways. Five methods were considered. Four of them were based on measurements, while the fifth was based on CFD calculations. The calibrations based on measurements used the natural wind for application of a reference wind direction. The first three methods use yawing of the stopped rotor for application of wind direction changes, while the fourth method referenced a met-mast mounted wind vane during operation.

5.1. Calibration of F_α method 1: forced yawing of wind turbine in stopped condition and use of tangent relation

Calibration method 1 use data acquired during a measurement campaign where the wind turbine rotor was stopped, and the rotor was yawed in and out of the wind (approximately $\pm 60°$) several times in order to gather a robust statistical database. The rotor azimuth position was assumed not to be important because of the internal calibration. However, it is

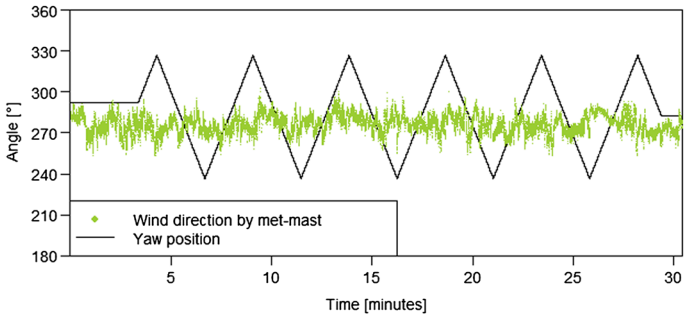

Figure 9. Wind direction at the met mast and yaw position during calibration.

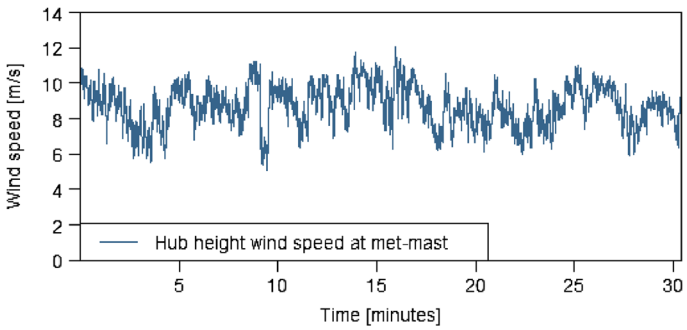

Figure 10. Wind speed at the met mast at hub height during calibration.

found appropriate that the rotor has a vertical symmetry (one blade pointing upwards or downwards) so that one spinner anemometer sonic sensor experiences constant wind while the other two experience variations in opposite directions.

During the calibration measurements, it is important that the wind direction is sufficiently stable (Figure 9). This is achieved by performing the measurements at wind speeds above 6 m s^{-1} to avoid high turbulence at low wind speeds,

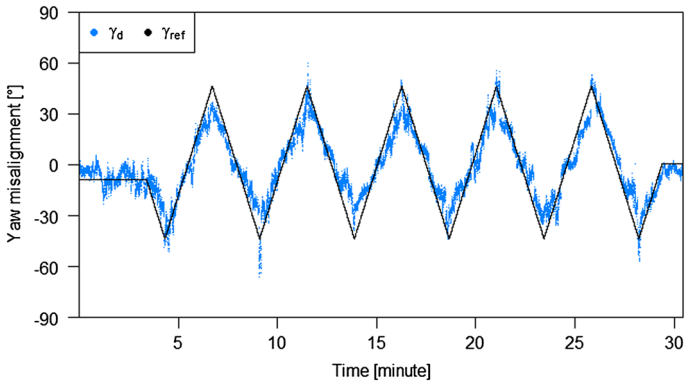

Figure 11. Non-calibrated time series of spinner anemometer and reference (corrected for average wind direction) yaw misalignment.

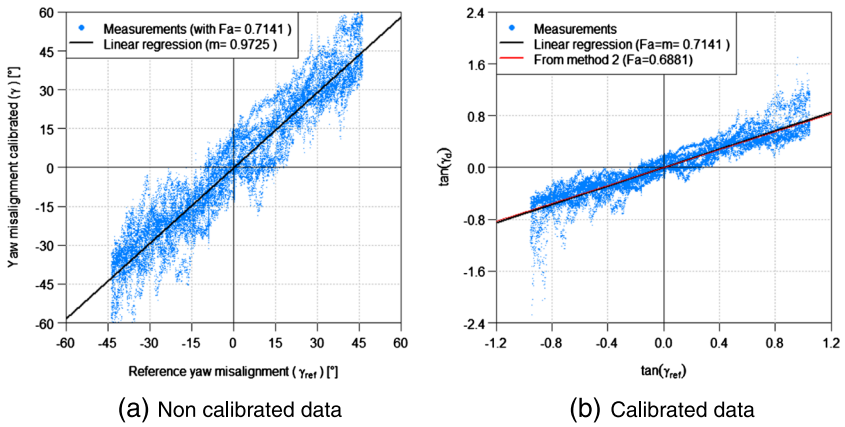

Figure 12. Reference and spinner anemometer data before and after calibration with method 1. (a) Non-calibrated data and (b) calibrated data.

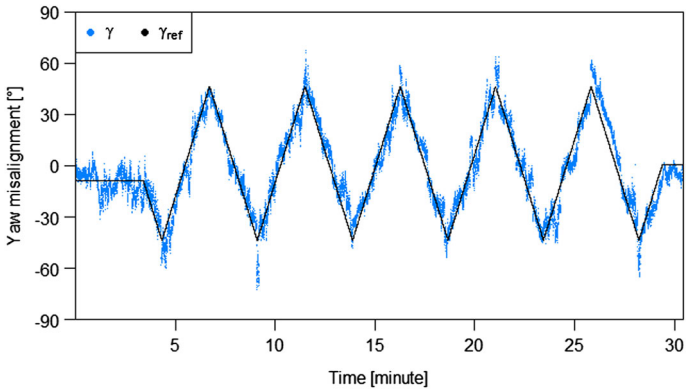

Figure 13. Calibrated time series of reference and spinner anemometer yaw misalignment data with method 1.

which normally increase the variability of the wind direction. Figure 10 shows the measured wind speed on the met mast during the calibration. The spinner anemometer data $U_{hor,d}$, γ_d and β_d, the rotor yaw direction θ_{yaw} and the met-mast data were sampled at 20 Hz during the measurements. The rotor yaw direction is now converted to a reference yaw misalignment with reference to the average wind direction: $\gamma_{ref} = \overline{\theta_{dir}} - \theta_{yaw}$. In Figure 11, the spinner anemometer yaw misalignment γ_d and the reference yaw misalignment γ_{ref} are plotted with time, and in Figure 12, the parameters are plotted against each other.

In order to use the tangent relations in equation (40), the reference yaw misalignment from Figure 9 must be offset to zero yaw misalignment with the averaged wind direction $\overline{\theta_{dir}}$. This was made with a linear regression between reference yaw misalignment data and default yaw misalignment measured by spinner anemometer. The offset was subtracted in Figures 11 and 12(a). Now, the tangent relation can be plotted, Figure 12(b), and a linear regression be made to find $F_\alpha = 0.7141$. The calibrated yawing is shown in Figure 13.

5.2. Calibration of F_α method 2: forced yawing of wind turbine in stopped condition and use of minimization procedure

Calibration method 2 used the same measurement procedure and database as method 1. For a calibrated instrument, where F_α has been found, the slope of the linear regressed line for the reference and calibrated yaw misalignments shall be equal to one (Figure 14(b)). This constraint is used to find the value of F_α with a minimization function $f(m) = |m - 1|$, where m is the slope of the linear regressed line of the reference and back and forth converted measured yaw misalignment data. The minimization routine utilizes a golden section search and successive parabolic interpolation on F_α. The back and forth conversion follows the procedure in Figure 6. The non-calibrated data are shown in Figure 14(a), while the calibrated data are shown in Figure 14(b), with $F_\alpha = 0.6881$.

5.3. Calibration of F_α method 3: forced yawing of wind turbine in stopped condition and use of direct expression

Calibration method 3 uses the same measurement procedure and database as methods 1 and 2. In method 3, F_α is found from a direct expression of F_α for each measured dataset with the tangent relation, (equation (40)). The default inflow angle to the rotor shaft axis α_d is found from the spinner anemometer output values through combination of the transformation equations derived in Section 3, considering also whether the default yaw misalignment γ_d is positive or negative:

$$\begin{aligned} \text{for } \gamma_d \geq 0 : \tan\alpha_d &= \frac{\sqrt{\sin^2\gamma_d + (\cos\gamma_d \sin\delta + \tan\beta_d cos\delta)^2}}{\cos\gamma_d \cos\delta - \tan\beta_d sin\delta} \\ \text{for } \gamma_d < 0 : \tan\alpha_d &= -\frac{\sqrt{\sin^2\gamma_d + (\cos\gamma_d \sin\delta + \tan\beta_d cos\delta)^2}}{\cos\gamma_d \cos\delta - \tan\beta_d sin\delta} \end{aligned} \tag{47}$$

The reference inflow angles are found from the rotor yaw direction measurements and calculated with equation (48). The reference yaw misalignment γ_{ref} is determined with the inverse transformation (Section 2.4). With a good approximation, one can set the reference flow inclination angle equal to the measured flow inclination angle with the default spinner anemometer constants: $\beta_{ref} = \beta_d$:

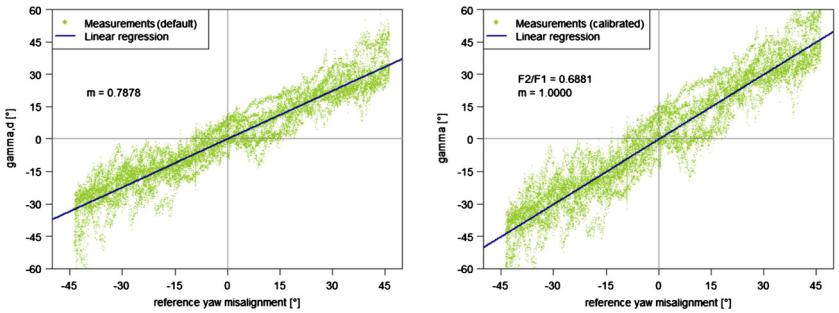

(a) Non calibrated data (b) Calibrated data

Figure 14. Reference and spinner anemometer yaw misalignment data before and after calibration with method 2. (a) Non-calibrated data and (b) calibrated data.

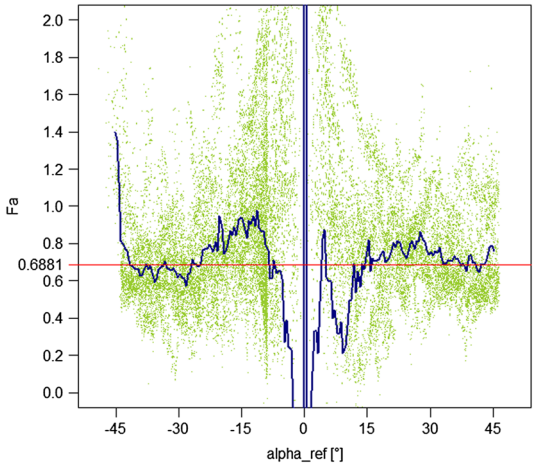

Figure 15. Method 3 yawing turbine in and out of wind in stopped condition and direct calculation of F_α. Red line is F_α from method 2 with the use of minimization function.

$$\text{for } \gamma_{ref} \geq 0 : \tan\alpha_{ref} = \frac{\sqrt{\sin^2\gamma_{ref} + \cos(\gamma_{ref}\sin\delta + \tan\beta_{ref} cos\delta)^2}}{\cos\gamma_{ref}\cos\delta - \tan\beta_{ref} sin\delta}$$
$$\text{for } \gamma_{ref} < 0 : \tan\alpha_{ref} = -\frac{\sqrt{\sin^2\gamma_{ref} + (\cos\gamma_{ref}\sin\delta + \tan\beta_{ref} cos\delta)^2}}{\cos\gamma_{ref}\cos\delta - \tan\beta_{ref} sin\delta} \tag{48}$$

Although F_α is expected to be constant for different inflow angles and wind speeds, the ratio $\tan\alpha_d/\tan\alpha_{ref}$ of equation (40) diverges significantly, see blue line in Figure 15. This is not appropriate for a robust determination of F_α, and thus, we will not present a result for this method.

5.4. Calibration of F_α method 4: use of met mast during operation and use of minimization procedure

Calibration method 4 utilizes a hub height wind direction measurement on a met mast together with measurement of rotor yaw direction to determine the reference yaw misalignment,[7] defined as the measured wind direction minus the rotor yaw direction:

$$\gamma_{ref} = \theta_{dir,10} - \theta_{yaw,10} \tag{49}$$

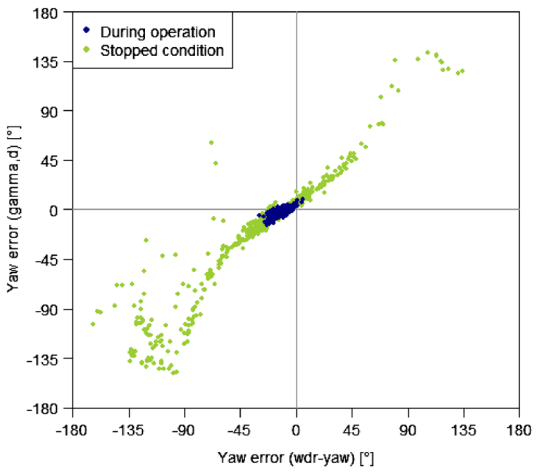

Figure 16. Method 4 calibration during operation with the use of met mast. Rotating (blue) and stopped (green).

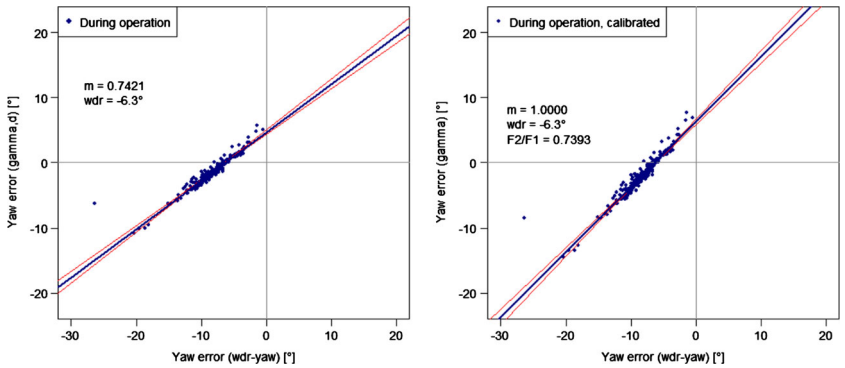

(a) Non-Calibrated data (b) Calibrated data

Figure 17. Yaw misalignment measurements during operation of the wind turbine with method 4, filtered for free wake sector and turbulence intensity less than 10% (red lines are linear fitting with *x*- and *y*-axis, while the blue line is the average). (a) Non-calibrated data and (b) calibrated data.

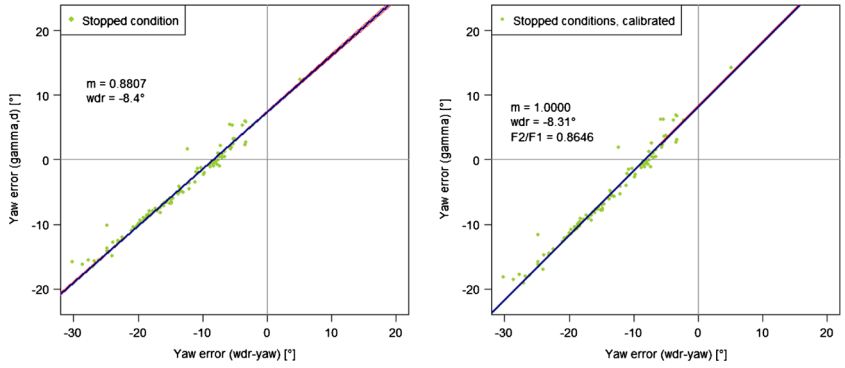

(a) Non-calibrated data (b) Calibrated data

Figure 18. Yaw misalignment measurements during stopped conditions of the wind turbine with method 4, filtered for free wake sector and turbulence intensity less than 10% (red lines are linear fitting with *x*- and *y*-axis, while the blue line is the average). (a) Non-calibrated data and (b) calibrated data.

Because of the physical distance between the met mast and the wind turbine, it is necessary to use 10 min averaging to ensure good correlation. This means longer time is required to acquire an appropriate database. The yaw misalignment measured by the spinner anemometer with default constants $k_1 = k_2 = 1$ versus mast-measured reference yaw misalignment is shown in Figure 16 (before filtering). The influence of the non-linearity of the spinner anemometer algorithm at reference yaw misalignments larger than $\pm 45°$ is clearly seen.

The measurements collected over 1 year were filtered for wind directions from 238° to 328° (free wake sector), for a turbulence intensity less than 10% and temperature above 2° to avoid icing conditions of the cup anemometer, resulting in 245 measurements during operation and 109 in stopped condition. Figure 17(a) shows a plot of uncalibrated spinner anemometer data during operation, while Figure 17(b) shows the corresponding calibrated data. Figure 18(b) shows a plot of uncalibrated spinner anemometer data in stopped conditions, while Figure 18(b) shows the corresponding calibrated data. Although filtering for a 90° sector, the measurements are seen to cover only a small range of yaw misalignment data. The minimization linear fitting procedure from method 2 is then used to find F_α. The results are $F_\alpha = 0.8646$ for stopped condition and $F_\alpha = 0.7393$ for operation.

5.5. Calibration of F_α method 5: use of CFD during operation and stopped

Calibration method 5 uses CFD for determination of F_α. The wind turbine rotor was modelled with the Ellipsys CFD software,[9–11] including detailed modelling of spinner, nacelle, blade roots and profiled blades. The flow was simulated for a free wind speed of 8 m s^{-1} and for inflow angles of 0°, 10°, 20°and 30°. For each inflow case, two simulations were

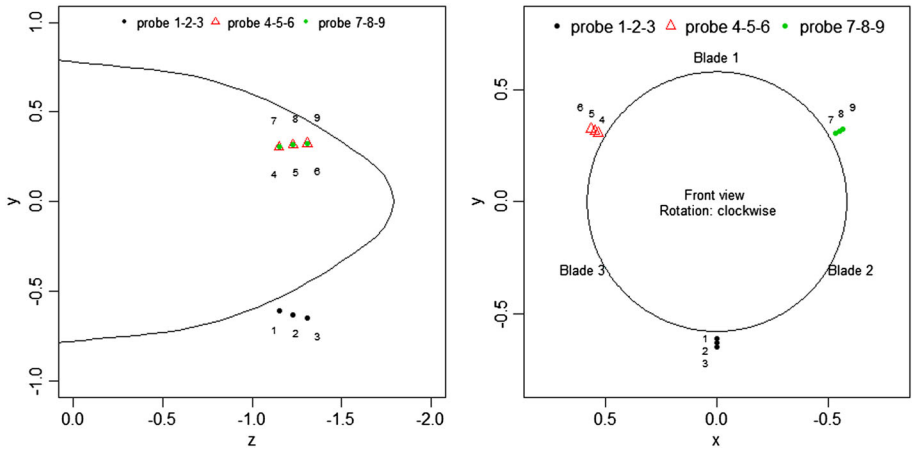

Figure 19. Side view and front view of spinner, indicating the coordinate system used for the CFD simulations (*x*-axis to the left, *y*-axis upwards, *z*-axis inwards along shaft axis).

performed, one with rotating rotor, the other with rotor stopped and blade number one pointing upwards ($\phi = 0°$). This gives eight test cases (rotating/stopped and four inflow angles). Tilt angle and flow inclination angles were set equal to zero; hence, the reference yaw misalignment corresponds to the inflow angle $\gamma_{ref} = \alpha_{ref}$.

The CFD simulation gives three velocity components (u, v, w) at three points along each sonic sensor path (nine points overall; Figure 19). For the non-rotating case, only one single rotor position was considered. For the rotating case, a full rotor rotation was divided into 2000 steps (0.18° each).

All the calculations consider the full rotor, with its blade profiles, over a simulation volume 10 times bigger than the rotor diameter. The simulation of the rotating cases also takes account of the induction due to the rotor at the spinner position.

In post-processing of the data, the components u, v, w in the global coordinate system were combined to a vector velocity $U(u, v, w)$. The vector of the sensor path $V(x, y, z)$ was calculated as the difference between the coordinates of the end points of the path and normalized to one. The sensor path wind speed was calculated as the dot product $U \cdot V$. The sensor path wind speeds and k_α for the rotating cases are shown in Figure 20 for 10°, 20° and 30°, respectively. k_α was calculated with equation (5) rearranged as

$$k_\alpha = \frac{k_2}{k_1} = \frac{\sqrt{3(V_1 - V_{ave})^2 + (V_2 - V_3)^2}}{\tan(\alpha_{ref})\sqrt{3}V_{ave}} \tag{50}$$

k_α was expected to be independent of rotor position, but unstable dynamic effects, dependent on rotor position and inflow angle, are seen to be pronounced, especially for greater inflow angles, as shown in Figure 20 to the right.

Figure 21 shows a summary of the nine k_α values for the different flow calculation cases.

The highest three values in Figure 21 are rotor averaged k_α values during rotation (black), while the points just below (red) are k_α values for rotor azimuth position $\phi = 0°$ of the same rotating case. The difference between the two cases (black and red points) does not represent a trend but is purely due to the variations of k_α over one revolution (Figure 20). The difference between the second case (red) and the third (blue) is small for the 10° inflow angle case, while the differences at 20° and 30° are in the order of about 15%.

6. DISCUSSION

A summary of the results of the five calibration methods to find F_α is shown in Table I.

The calibration measurements and simulations were made for both operating and stopped conditions.

Method 1 with forced yawing and high sampling rate in stopped condition is a robust procedure that is easy and fast to perform in the field. The yaw misalignments can be forced to reasonably high values, which is also necessary because the spreading of data due to variations in wind direction during measurements is high. The resulting calibration factor $F_\alpha = 0.7141$ is 7% higher than for the CFD calculation at 10° inflow angle. F_α for higher flow angles of the CFD calculations are somewhat smaller (up to 20%).

Method 2 using a minimization function to achieve correct slope gave a result close to method 1 (3% lower). The two methods are quite similar. Method 2 is a little more cumbersome as a minimization, and iterative procedure is needed while method 1 is more direct.

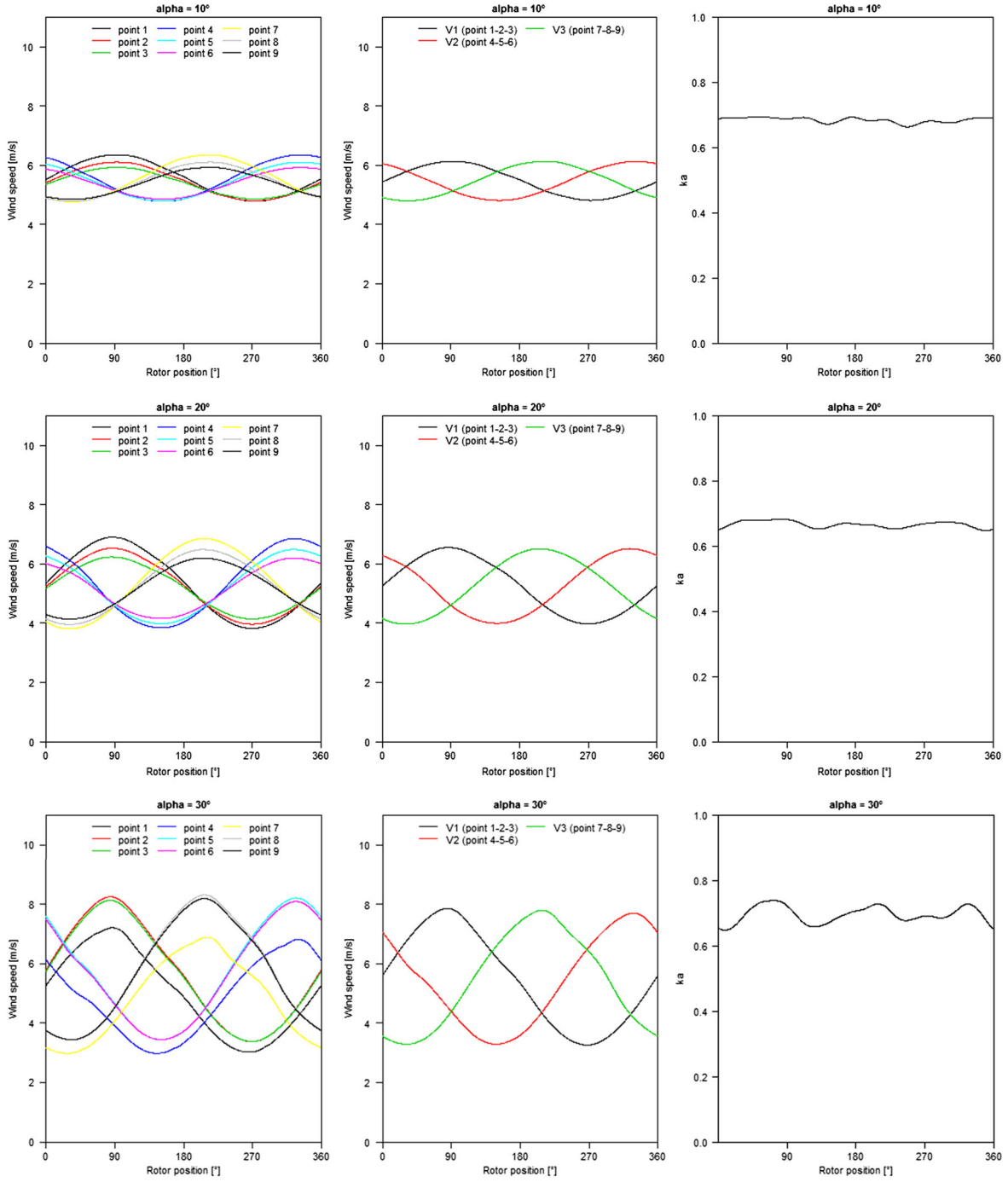

Figure 20. The CFD calibration simulations during rotation, method 5, for $\alpha = 10^{\circ}, 20^{\circ}$ and 30° from top to bottom. Wind speeds along sonic sensor paths to the left, averaged wind speeds in the middle and k_{α} to the right.

Method 3 using the direct expression of F_{α} seemed to fail to give useful results. Especially, the large variations of F_{α} in the range $\pm 15^{\circ}$ is disappointing. The singularity at 0° was expected, but the influence in the surroundings of the singularity is spoiling the method.

Method 4 used 10 min averages recorded during normal operation and in stopped condition. The 10 min averaging ensures reasonably robust measurement points, but the yaw misalignment range during operation is rather small. For stopped condition, F_{α} is significantly larger than for operating condition (about 17%), and it is also significantly larger than the value for methods 1 and 2 (about 20%).

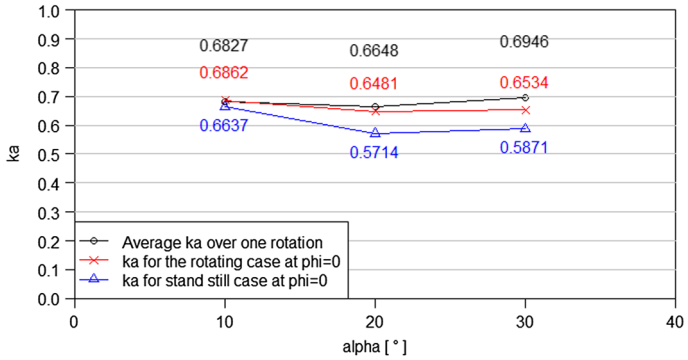

Figure 21. Calibration coefficient from different CFD simulation cases; rotating and averaged (black), rotating at $\phi = 0^{\circ}$ (red), stopped at $\phi = 0^{\circ}$ (blue).

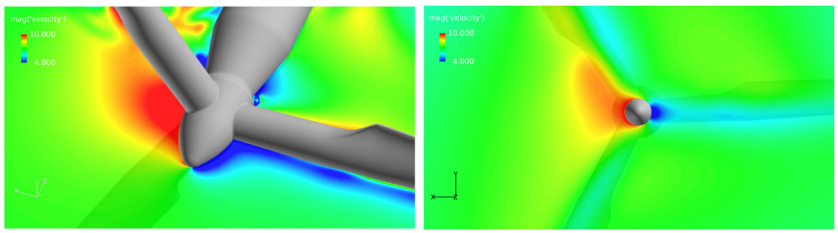

Figure 22. Graphic presentation of a CFD result for 8 m s^{-1} and inflow angle $\alpha_{ref} = 30^{\circ}$ from the right, rotor position $\phi = 90^{\circ}$ (blade 1 horizontal). (a) Wind speed in horizontal plane seen from above and (b) wind speed in vertical plane at $z = -1.15$.

Table I. Summary of results of calibration methods for angular measurements.

Method	Test method description	Analysis to determine F_{α}	F_{α}	Condition
Method 1	Forced yawing of wind turbine with stopped rotor, acquisition of data from spinner anemometer and yaw direction at 1 Hz or faster at wind speed >6 m s^{-1}	Correction of data for average wind direction, plotting data with tangent relations and linear regression	0.7141	Stopped
Method 2	Same as method 1	Minimization of slope function with golden search and successive parabolic interpolation routine using back and forth conversions	0.6881	Stopped
Method 3	Same as method 1	Direct calculation of F_{α}	0.6–1.0	Stopped, high scatter
Method 4	Acquisition of 10 min averaged data from spinner anemometer, yaw direction and met mast over months long period	Operation and stopped data from condition of wind turbine analysed separately.	0.8646 0.7393	Stopped Operating
Method 5	Full rotor CFD simulation for different inflow angles, for rotating and non-rotating conditions	Post-processing of three-dimensional wind field to calculate sensor path wind speeds and F_{α} with forward transformation	0.6637 0.5714 0.5871 0.6862 0.6481 0.6534 0.6827 0.6648 0.6946	Stopped, $\alpha = 10^{\circ}, \phi = 0^{\circ}$ Stopped, $\alpha = 20^{\circ}, \phi = 0^{\circ}$ Stopped, $\alpha = 30^{\circ}, \phi = 0^{\circ}$ Operating, $\alpha = 10^{\circ}, \phi = 0^{\circ}$ Operating, $\alpha = 20^{\circ}, \phi = 0^{\circ}$ Operating, $\alpha = 30^{\circ}, \phi = 0^{\circ}$ Operating, $\alpha = 10^{\circ}, \phi = ave$ Operating, $\alpha = 20^{\circ}, \phi = ave$ Operating, $\alpha = 30^{\circ}, \phi = ave$

The difference in F_α from stopped to operating might be due to induced wind speed from the operating and thrust-generating rotor. The induced wind speed reduces the longitudinal component U_x, while the transversal component U_y is the same. The effect is that the local yaw misalignment at the spinner is larger than in the far field. With a known induction function $a(U) = (U_\infty - U)/U_\infty$, the correction of locally measured yaw misalignment to the far field is

$$\gamma_\infty = \arcsin((1 - a) \sin \gamma) \tag{51}$$

For a yaw misalignment measured at the spinner of 10° and an induction factor of 10%, the yaw misalignment measured at the far field is 9.0° (10% lower). When a yaw misalignment at the spinner is higher during operation than when stopped, then the F_α value for operating condition should be higher than for stopped condition. Method 4 in Table I shows the opposite. This is a controversy. However, the measurements in stopped condition are made during operating periods of the wind turbine. Stopped conditions do only occur for very low wind speeds where the wind turbine stops or is idling because of low wind conditions. The measurements for stopped conditions are thus far from the requirements in methods 1–3 of wind speeds above 6 m s^{-1}. The stopped condition measurements of method 4 should therefore be considered with reservation. The measurements during operation comply well with the measurements in stopped condition of methods 1 and 2 considering a calculated induction factor in the range 2.5% to 7.4%, using equation (51). This level of the induction factor is, however, lower than what should be expected. A reason for an increased uncertainty in use of method 4 is the quite small yaw misalignment range during operation.

Method 5 with CFD simulations results in quite some variety. Figure 20 shows increasing variability of k_α over a rotation with increasing inflow angle. The variability pattern is without a 3P similarity. This indicates fluctuations in the aerodynamic flow over the spinner or unsteadiness in the CFD calculations. The wind speed flow pattern in Figure 22(b) indicates flow separation at the spinner nose at 30° inflow angle. At lower inflow angles, Figure 20 right, the variability is reduced. The most trustworthy calibration values with CFD for angular measurements must therefore be found in the 10° inflow angle simulations, as this is the area where actual yaw misalignment measurements are expected. For stopped condition, k_α is significantly higher for 10° inflow angle than for 20° or 30°. For operating condition, k_α is 3.4% higher for 10°, while it is 11–13% for 20° to 30°.

Overall, methods 1 and 3, with quite comparable results, are in good agreement with method 4 for operating conditions, with a calculated increase in k_α of 3.5% for operating conditions due to induction. This is equivalent to CFD simulations for 10° inflow angle with an increase of 3.5% due to induction. The CFD simulations just give k_α values about 8% lower values than field calibrations, as seen in Table I. The reason for the lower k_α values from CFD simulations might be due to calculation uncertainties connected with flow separation on the spinner nose because of the pointed spinner. This might be a disadvantage specifically on this type of spinner and might not be found on more rounded spinners.

6.1. Uncertainty of yaw misalignment measurements

Angular measurements with the spinner anemometer has some uncertainties connected to calibration as well as some other relations. The influence of induced wind speeds raises the question whether the measured yaw misalignment is defined as a local inflow angle at the spinner or a far field inflow angle. We find it most appropriate to define the yaw misalignment as a local inflow angle, as well as we find it most appropriate to define the measured wind speed as a local wind speed. The induction function, as mentioned earlier, should be used to correct the measurements to the far field. The induction function should be found as part of the calibration of F_1. This could be made according to the International Electrotechnical Commission standard,[8] as a determination of the nacelle transfer function. Defining the yaw misalignment as a local measurement reduces the uncertainty because of a clear definition of the measurand. Calibration methods 1 and 2 are therefore also the preferred methods.

The sonic sensors must always be zero wind calibrated, as they are from factory. A traceable wind tunnel calibration could be made if required, but this should normally not be necessary for angular measurements because the uncertainty is relatively low. The internal calibration must be made prior to calibration for angular measurements to smooth out variations during each rotation, so that the rotor azimuth position during calibration yawing does not influence on the calibration. The uncertainty related to the calibration factor F_α with methods 1 and 2, where we have taken the non-linearity of the spinner anemometer algorithm into account, is estimated at ±2%, for use of either of the two methods and a linearization uncertainty with a standard deviation of 10%. The uncertainty of the yaw direction sensor is estimated at ±2°. However, the uncertainty on the linearity is estimated to be close to zero, so we do not need to take this into account. If we assume rectangular uncertainty distributions for use of methods 1 or 2 and linearization, and combine the uncertainty components, we get a standard uncertainty of 10% of F_α.

The uncertainty of F_α, and thus k_α, provides an uncertainty of α of the same order. The yaw misalignment and flow inclination angles are directly derived from α and have the same uncertainty connected to them. A spinner anemometer that measures for example 10° yaw misalignment, and where the standard uncertainty of F_α is 10%, will have a standard uncertainty on the yaw misalignment of 1°.

7. CONCLUSIONS

In the first part, the spinner anemometer conversion algorithm that converts the measured wind speeds by the sonic sensors to horizontal wind speed, yaw misalignment and flow inclination angle is described. The inverse conversion is derived in order to use earlier measured wind data (measured with default constants k_1 and k_2) to find the calibration factor F_α. F_α is used to correct the default spinner anemometer ratio $k_{\alpha,d} = k_{2,d}/k_{1,d}$ to the calibrated ratio $k_\alpha = k_2/k_1$ by $k_\alpha = F_\alpha k_{\alpha,d}$. It was found that F_α was the only single calibration factor that angular measurements depend on. It was further found that calibration for angular measurements should be made after internal calibration of the spinner anemometer and before wind speed calibration.

Five different methods for calibration of a spinner anemometer for yaw misalignment measurements were presented for a stall-regulated 500 kW wind turbine with a spinner anemometer mounted on a pointed spinner. The first three calibration methods 1–3 consist of stopping the turbine in a steady and low turbulent wind (>6 m s^{-1}) and yawing the turbine several times in and out of the wind. These methods used fast-sampled measurements (20 Hz, >1 Hz). Time required was about half an hour. Method 1 used a tangent relation with a linear regression to find $F_\alpha = 0.7141$ and was the highest recommended method with method 2 using a minimization function and an iterative process with back and forth conversion algorithms to find $F_\alpha = 0.6881$, following very close. Method 3 failed to give a satisfactory result.

Method 4 used 10 min average data during normal operation and standstill of the wind turbine, combined with wind direction measurements from a met-mast upwind of the wind turbine. Data for stopped condition were found to be made at too low wind speeds. For operation condition, we found $F_\alpha = 0.7393$. The higher value than for methods 1 and 2 was assumed to be due to rotor induction.

Method 5 used CFD to calculate the flow over the spinner for axial and skew airflow during operating and stopped conditions. F_α was found directly from the calculations. The calculations for 10° inflow angle were considered to be the most trustworthy, deriving F_α values approximately 8% lower than for field calibrations. The differences were considered to be due to separation on the pointed spinner.

The influence of rotor induction increases the yaw misalignment measurements locally at the spinner compared with the far field. We define the yaw misalignment measurements to be a local measurement; therefore recommending calibrations by yawing the wind turbine in and out of the wind in stopped conditions and eventually using an induction function for correction to the far field. The uncertainty connected with the calibration was found to be approximately 10%, resulting in an uncertainty of 1° for a 10° yaw misalignment measurement.

ACKNOWLEDGEMENTS

This work was performed as part of an EUDP project funded by the Danish Energy Agency and by Vattenfall, Metek and Vestas. (J.nr 64009-0273). The authors would like to thank the people from Metek, Vattenfall and ROMO Wind for the help with technical support and for their good collaboration in the project.

REFERENCES

1. Frandsen S, Sørensen N, Mikkelsen R, Pedersen TF, Antoniou I, Hansen K. The generics of wind turbine nacelle anemometry. *EWEC 2009*, Bruxelles, 2009.
2. Zahle F, Sørensen NN. Characterization of the unsteady flow in the nacelle region of a modern wind turbine. *Wind Energy* 2011; **14**: 271–283.
3. Højstrup J, Nielsen D, Hansen K, Lauritzen L. Maximise energy production by minimizing yaw misalignment. Large scale field deployment of spinner anemometer. *Poster 0162, EWEC 2013*, Vienna, 2013.
4. Pedersen TF. Spinner anemometer—an innovative wind measurement concept. *EWEC 2007*, Milan, 2007.
5. Pedersen TF, Sørensen N, Evevoldsen P. Aerodynamics and characteristics of a spinner anemometer. *Journal of Physics: Conference Series 75 012018* 2007.
6. Spinner anemometer user manual version 9.27-3. *Metek Meteorologische Messtechnik GmBH*, Germany, 2012.
7. Paulsen US, *Vindmølleafprvning Nordtank NTK 500/41, Måling af Effektkurve*, Technical Report Risø-I-889 DA, Risø National Laboratory, Roskilde, Denmark, November 1995.
8. IEC 61400-12-2 Wind turbines - part 12-2: Power performance of electricity producing wind turbines based on nacelle anemometry, Edition 1.0, 2013-03.
9. Michelsenl JA, Basis3D–a platform for development of multiblock PDE solvers. *Technical Report AFM 92-05*, Technical University of Denmark, 1992.

10. Michelsen JA, Block structured multigrid solution of 2D and 3D elliptic PDEs. *Technical Report AFM 94-06*, Technical University of Denmark, 1994.
11. Sørensen NN, General purpose flow solver applied to flow over hills. *Technical Report Risø-R-827(EN)*, Risø National Laboratory, 1995.

DOI: 10.1002/we